



CM-P00057435

Preliminary note I.

on

Particle production in 6.2 GeV (kin.lab)  
P-P collisions treated by a statistical model

F. Cerulus and R. Hagedorn

CERN, Geneva

The Fermi theory of particle production is used in an exact and refined form in order to calculate various quantities for 6.2 GeV primary kinetic energy P-P-collisions.

The probability for a certain final state  $b$  is in the Fermi model :

$$P_b = W_{\alpha\beta\gamma}^{(b)}(T) \left\{ \frac{\pi (2S_j + 1)^{\sigma_j}}{\pi N_i!} \right\} \Omega^{n-1} \rho_b^*(E, m_1, \dots, m_n, \vec{p} = 0)$$

here  $W_{\alpha\beta\gamma}^{(b)}(T)$  is the number of linearly independent isospin eigenfunctions of total isospin  $T$  and fixed but arbitrary  $T_3$ , which can be built up with  $\alpha$  particles of isospin  $1/2$ ,  $\beta$  particles of isospin  $1$  and  $\gamma$  particles of isospin  $3/2$ .

The next factor counts the multiplicities of ordinary spin where  $\sigma_j$  is the number of particles of spin  $S_j$ , the product  $N_i!$  stays for the indistinguishability of the particles.  $\Omega^{n-1}$  is the so called interaction volume and  $\rho_b^*(E, m_1, \dots, m_n)$  is the phase space density of the final state :

$$\rho_b^*(E, m_1, \dots, m_n, \vec{p}) = \int d\vec{p}_1 \dots d\vec{p}_n \delta(E - \sum \sqrt{p_i^2 + m_i^2}) \delta(\sum \vec{p}_i - \vec{p})$$

Also the energy spectrum of a particle in CM is given essentially by  $\mathcal{P}^*$ , namely e.g. for the particle  $m_n$ :

$$w_n(p) dp \sim 4\pi p^2 dp \cdot \mathcal{P}^*(E - \sqrt{m_n^2 + p^2}, m_1 \dots m_{n-1}, \vec{p} = -\vec{p}_n)$$

We have a Monte Carlo method (Described in Suppl. Nuovo Cimento, Vol.9, 646 (1958)), which allows us to calculate such integrals with any prescribed accuracy and we choose the accuracy such that the results given below are

exact within less than  $\pm 1\%$  for the particle numbers  
 " " " "  $\pm 3\%$  for the spectra

In particular, the influence of small differences in the masses, e.g.  $\sum$  and  $\Delta$  shows up clearly far outside the statistical error.

We have considered all reactions at this energy, which contribute to the observable final states and give a list of them below (Table 1).

For all these reactions  $P_b$  has been calculated with the above formula and then the spectra of the different kinds of particles which come out from the Monte Carlo calculation in normalized form

$$\int w(\varepsilon) d\varepsilon = 1$$

are multiplied by  $P_b$  and by the number of particles  $n_i^{(b)}$  which are represented by  $W_i(\varepsilon)$  in the reaction considered:

$$W_i^{(b)}(\varepsilon) = P_b \cdot n_i^{(b)} \cdot w_i^{(b)}(\varepsilon) \quad i = \text{kind of particle} \\ b = \text{kind of reaction}$$

Finally, they are added up for each kind of particle :

$$W_i(\varepsilon) = \sum_b P_b n_i^{(b)} w_i^{(b)}(\varepsilon)$$

which is the not-normalized total spectrum of particle  $i$ . We have then, since  $w_i^{(b)}(\varepsilon)$  is normalized

$$\int W_i(\varepsilon) d\varepsilon = \sum_b P_b n_i^{(b)} = \langle n_i \rangle \cdot \sum_b P_b$$

Here  $\langle n_i \rangle$  is the mean absolute particle number per collision - averaged properly weighted over all reactions.

Finally, the normalized total spectrum  $i$  and the mean kinetic energy is calculated.

#### Refinements :

We have, however, made a few refinements which seem to be essential :

- 1) We include the formation of the isobar ( $T=3/2$ ,  $S=3/2$ ) which afterwards decays into  $N + \bar{\pi}$ .
- 2) We include final state annihilation of  $N - \bar{N}$  -pairs by saying that they will annihilate, if they come out with a small momentum relative to each other and thus stay for some time near to each other. We assumed that the probability for annihilation is given by

$$\left[ \text{probability for a certain relative momentum, } p \right] \text{ times} \\ \left[ \text{probability for annihilation when the rel.momentum is } p \right]$$

The first factor is calculated by means of the phase-space by simulating a  $N - \bar{N}$  -pair with relative momentum  $p$  by one particle of mass

$$m^* = 2M_N + \frac{p_{\text{rel}}^2}{2M} ,$$

the second factor is taken to be

$$\frac{\sigma_{\text{annihil}}}{\sigma_{\text{total}}} (p_{\text{rel}})$$

calculated with the help of a simple model with complex potential, which represents fairly well the data for  $\bar{P}P$ -scattering.

The number of annihilating pairs at a given reaction  $b$  turns then out to be proportional to

$$\text{const.} \int_0^{p_0} \frac{\sigma_{\text{annihil}}}{\sigma_{\text{total}}} \cdot p_{\text{rel}}^2 \cdot f^*(E, m_1, \dots, m_{n-1}, m^*(p_{\text{rel}})) dp_{\text{rel}}$$

This has then to be subtracted from the number of pairs which the primary interaction yields. In a similar way the  $\bar{N}$ -spectrum is changed, in particular the low energy part of it is reduced as it is to be expected from this model of final state annihilation.

We give below the original  $\bar{N}$ -spectrum, the  $\Delta \bar{N}$ -spectrum, that is: the spectrum of the annihilating  $\bar{N}$  and the observable spectrum  $\bar{N} - \Delta \bar{N}$ .

In the yield of  $\bar{N}$  this final state annihilation gives a reduction by a factor two roughly.

3) We consider a third rather trivial final state interaction by calculating the spectra of  $\gamma$  and  $\Lambda^0$  from the decays :

$$\pi^0 \rightarrow 2\gamma$$

$$\Sigma^0 \rightarrow \Lambda^0 + \gamma$$

and by adding up all such  $\gamma$ -spectra and adding this  $\Lambda^0$  to those produced directly.

4) The interaction volume is split into three :

$$\Omega^{n-1} \rightarrow \Omega_1^{n_1} \cdot \Omega_2^{n_2} \cdot \Omega_3^{n_3}$$

where now

$$n_1 = \text{number of } \pi + N + \bar{N}$$

$$n_2 = \text{number of } \Lambda + \Sigma + \Xi$$

$$n_3 = \text{number of } K$$

We calculated now everything in several versions, namely

$$(i) \quad \Omega_1 = \Omega_2 = \Omega_\pi = \frac{4\pi}{3} \lambda_\pi^3$$

$$\Omega_3 = \Omega_K \text{ variable}$$

$$(ii) \quad \Omega_1 = \Omega_\pi$$

$$\Omega_2 = \Omega_3 = \Omega_K \text{ variable}$$

Assumption (i) seems to represent global symmetry whereas assumption (ii) treats the hyperons and K-mesons equally.

If one considers  $\Omega$  as an expression of the coupling strength, then one should expect  $\Omega_K$  to be 10-15 times smaller than  $\Omega_\pi$ .

If, on the other hand, one interprets it as expressing ranges of interactions, then  $\Omega_K$  should be the same expression as  $\Omega_\pi$  but with  $\lambda_K$  replacing  $\lambda_\pi$ . Then it should be about 40 times smaller than  $\Omega_\pi$ .

The meaning of  $\Omega$  being obscure, we varied  $\Omega_K$  from  $\Omega_K = \Omega_\pi$  down to  $\Omega_K^0 \approx 1/50 \Omega_\pi$  and that in both versions (i) and (ii).

The curves given below show then the effect of this variation.

It is interesting to see that there are certain quantities which depend strongly neither on  $\Omega_K$  nor on which of (i) or (ii) is taken, e.g. the total  $\gamma$ ,  $\bar{N}$ ,  $\pi$ -production, whereas others depend very strongly, changing by orders of magnitude.

The normalized spectra are hardly influenced and can be said to be independent of the version taken.

Further explanations will be found in the figure captions.

Angular distribution :

In this kind of model nothing is known concerning angular distribution, in fact, isotropy is tacitly assumed. It is believed however, that the spectra given are not bad if they are considered as averaged over all angles in the CM.

Concluding remarks :

The present calculation shows that the Fermi model, taken seriously, is everything else than a simple model. It was possible to perform this calculation only with the help of an electronic computer (CERN's Ferranti Mercury).

We got the impression that the model may very well be able to reproduce many experimental facts - except angular distribution - and that the discrepancies encountered so far (up to  $\lesssim 50$  GeV) lie not in the model but in the fact that it has not been used correctly; may that concern very bad approximations for the phase space or the omission of the other factors, which easily become of the order of 1/100 or may it come from considering only a small subset of all possible and contributing reactions at a given energy.

Certainly the final state interactions play an important rôle also.

Exact calculations at 10 and 25 GeV and on  $N-\bar{N}$  annihilation are on the way, results at 2.75 GeV have been published already (CERN-59-3).

We would like very much to receive comments and experimental results to compare with.

TABLE 1.

The initial state is always P+P, the final states are listed below together with their probabilities in per cent of the total cross-section (which cannot be calculated by this theory). We give two versions :

$$(\alpha) \quad \Omega_1 = \Omega_2 = \Omega \quad ; \quad \Omega_3 = \frac{1}{8.5} \Omega \text{ (global symmetry)}$$

$$(\beta) \quad \Omega_1 = \Omega_\pi \quad ; \quad \Omega_2 = \Omega_3 = \frac{1}{8.5} \Omega_\pi$$

(The value 1/8.5 is purely accidental - it just happened that this was one of the values for which everything was calculated in order to draw the curves of Figs. 13-21. This value, however, is the nearest to 1/10, which we would consider reasonable. Anyway, the difference is unimportant).

We neglected all those reactions which, within a group of similar reactions, are very improbable, with respect to the others of the same group, with some exceptions : These exceptions have no influence at all, we list them for curiosity only.

Notation  $1.09, \pm 5$  means  $1.09 \times 10^{-5}$  etc.

TABLE 1. Reactions considered.

Reactions	Prob. in %: ( $\alpha$ )	( $\beta$ )
2N (elastic, incoherent)	1.32, -1	1.41, -1
2N+ $\pi$	4.59, +0	4.88, +0
2N+2 $\pi$	1.09, +1	1.16, +1
2N+3 $\pi$	5.51, +0	5.80, +0
2N+4 $\pi$	8.23, -1	8.74, -1
2N+5 $\pi$	3.70, -2	3.93, -2
$N^*+N \rightarrow 2N+\pi$	5.01, -1	5.32, -1
$N^*+N+\pi \rightarrow 2N+2\pi$	1.08, +1	1.15, +1
$N^*+N+2\pi \rightarrow 2N+3\pi$	2.43, +1	2.58, +1
$N^*+N+3\pi \rightarrow 2N+4\pi$	8.70, +0	9.24, +0
$N^*+N+4\pi \rightarrow 2N+5\pi$	6.92, -1	7.35, -1
$N^*+N+5\pi \rightarrow 2N+6\pi$	1.91, -2	2.03, -2
2N* $\rightarrow 2N+2\pi$	4.70, -1	5.00, -1
2N*+ $\pi$ $\rightarrow 2N+3\pi$	1.06, +1	1.13, +1
2N*+2 $\pi$ $\rightarrow 2N+4\pi$	1.21, +1	1.29, +1
2N*+3 $\pi$ $\rightarrow 2N+5\pi$	2.55, +0	2.71, +0
2N*+4 $\pi$ $\rightarrow 2N+6\pi$	1.05, -1	1.12, -1
2N*+5 $\pi$ $\rightarrow 2N+7\pi$	1.13, -3	1.20, -3
3N+ $\bar{N}$ (without final state annihil.)	9.46, -3	1.00, -2
$\Lambda +N+K$	3.43, -1	4.28, -2
$\Lambda +N+K+\pi$	8.21, -1	1.08, -1
$\Lambda +N+K+2\pi$	2.81, -1	3.50, -2
$\Lambda +N+K+3\pi$	1.77, -2	2.21, -3
$\Lambda +N^*+K \rightarrow \Lambda +N+K+\pi$	4.23, -1	5.26, -2
$\Lambda +N^*+K+\pi \rightarrow \Lambda +N+K+2\pi$	5.68, -1	7.06, -2
$\Lambda +N^*+K+2\pi \rightarrow \Lambda +N+K+3\pi$	1.04, -1	1.30, -2
$\Lambda +N^*+K+3\pi \rightarrow \Lambda +N+K+4\pi$	2.38, -3	2.96, -4
$\Sigma +N+K$	5.49, -1	6.83, -2
$\Sigma +N+K+\pi$	1.30, +0	1.61, -1
$\Sigma +N+K+2\pi$	3.45, -1	4.29, -2
$\Sigma +N+K+3\pi$	2.14, -2	2.67, -3
$\Sigma +N^*+K \rightarrow \Sigma +N+K+\pi$	6.62, -1	8.24, -2
$\Sigma +N^*+K+\pi \rightarrow \Sigma +N+K+2\pi$	9.98, -1	1.24, -1
$\Sigma +N^*+K+2\pi \rightarrow \Sigma +N+K+3\pi$	1.16, -1	1.44, -2
$\Sigma +N^*+K+3\pi \rightarrow \Sigma +N+K+4\pi$	2.47, -3	3.08, -4
$\Xi +N+2K$	1.30, -2	1.61, -3
$\Xi +N+2K+\pi$	1.39, -3	1.73, -4
$\Xi +N+2K+2\pi$	1.09, -5	1.36, -6
$\Xi +N+2K+3\pi$	3.64, -9	4.54, -10
$\Xi +N^*+2K \rightarrow \Xi +N+2K+\pi$	2.76, -3	3.43, -4
$\Xi +N^*+2K+\pi \rightarrow \Xi +N+2K+2\pi$	3.04, -5	3.79, -6
$\Xi +N^*+2K+2\pi \rightarrow \Xi +N+2K+3\pi$	7.06, -10	8.78, -11
2N+K+ $\bar{K}$	6.60, -2	7.01, -2
2N+K+ $\bar{K}+\pi$	3.45, -2	3.66, -2
2N+K+ $\bar{K}+2\pi$	2.11, -3	2.24, -3
2N+K+ $\bar{K}+3\pi$	2.48, -5	2.64, -5
$N^*+N+K+\bar{K} \rightarrow 2N+K+\bar{K}+\pi$	8.15, -2	8.65, -2
$N^*+N+K+\bar{K}+\pi \rightarrow 2N+K+\bar{K}+2\pi$	1.66, -2	1.77, -2
$N^*+N+K+\bar{K}+2\pi \rightarrow 2N+K+\bar{K}+3\pi$	2.98, -4	3.16, -4
$N^*+N+K+\bar{K}+3\pi \rightarrow 2N+K+\bar{K}+4\pi$	3.71, -7	3.94, -7
$2N^*+K+\bar{K} \rightarrow 2N+K+\bar{K}+2\pi$	1.65, -2	1.75, -2
$2N^*+K+\bar{K}+\pi \rightarrow 2N+K+\bar{K}+3\pi$	6.42, -4	6.82, -4
$2N^*+K+\bar{K}+2\pi \rightarrow 2N+K+\bar{K}+4\pi$	3.43, -7	3.65, -7

Explanations for figures 1 - 12 (spectra).

All spectra represent kinetic energies in the centre of mass system of the colliding protons. They are normalized to unity. The quantity represented is the ratio:

$$\frac{\text{number of particles } n(\mathcal{E}) \text{ per energy interval}}{\text{mean total number } \langle n \rangle \text{ of particles of that kind}}$$

The energy interval was chosen to be 50 MeV except for the anti-nucleons, where it is 1 MeV.

The points are the resulting values from the above described weighted superposition of the Monte Carlo spectra. Some spectra are represented very smoothly, namely those to which many of the reactions listed in Table 1 contribute (e.g.  $\pi$ -spectra). Some others show still large fluctuations (e.g.  $\bar{N}$ ). The solid curves are partly drawn by hand and partly found by a least square fit by a Fourier series of  $\sin v\mathcal{E}$ ,  $v = 1 \dots 5$ . The curves are statistically more accurate than the points and their error is probably of the order of - or less than - about 3%, for some curves much better. The amount of scattering of the drawn in points gives a qualitative feeling for the goodness of fit of the curve.

Explanations for figures 13 - 21.

Here the mean values of absolute particle numbers per collision and some ratios of such numbers are shown for each kind of particle. We made no attempt to divide them up for the different charges. Roughly, but not exactly, the numbers of  $\pi^+ : \pi^0 : \pi^-$  will be  $1 : 1 : 1$  and analogously for  $\Sigma$ , N. But for cases in which very few particles are produced, this is certainly wrong. If in experimental analysis one classifies events according to the number

of prongs, then one has to be very careful. (See F. Cerulus and R. Hagedorn, CERN 59-3, where the charge distribution at another energy is carried through. Essentially the same has to be done in the present case, but this amounts to a fairly large calculation.)

In all figures  $\Omega_K$  is the varying variable and the curves show the dependence of the particle numbers on  $\Omega_K$ . In all cases where the assumptions

$$(i) \quad \Omega_Y = \Omega_\pi \quad \text{and}$$

$$(ii) \quad \Omega_Y = \Omega_K$$

show different results, two curves are given. When only one curve is drawn, it means that both assumptions lead to the same result.

Obviously both assumptions give the same result for those quantities, which anyway hardly change with  $\Omega_K$ , namely, the numbers of  $\pi$ ,  $N$ ,  $\bar{N}$  and  $\chi$  from  $\pi^0$  and  $\Sigma^0$  decay. There we show these numbers in a linear scale.

The numbers of hyperons and K-mesons depend strongly on  $\Omega_K$  and that differently for either assumption, they are shown in a logarithmic scale.

We would expect that assumption (i)  $\Omega_Y = \Omega_\pi$  with a value of  $\Omega_K$  between  $1/10 \Omega_\pi$  and  $1/15 \Omega_\pi$  should give agreement with experiments. This would agree in a loose sense with global symmetry and a coupling strength for the K-mesons which is smaller by about one order of magnitude than that of the  $\pi$  mesons.

Figure captions.

Fig. 1 to Fig. 12 - Captions will be found on the figures.

Fig.13 Mean number of  $\pi$  and  $N$  per collision.

Fig.14 Mean number of  $\bar{N}$  per collision.

Fig.15 Ratio of  $\pi^-/\bar{p}$ .

Fig.16 Total  $\chi$  number from  $\pi^0$  and  $\Sigma^0$  decay per collision.

Fig.17 Total  $\Sigma$  and  $\Lambda$  number per collision. It is interesting to note that the total number of  $\Sigma^+, \Sigma^0, \Sigma^-$  equals the total number of  $\Lambda$ , where the latter is  $\Lambda_{\text{direct}} + \Lambda_{\text{from } \Sigma^0}$ . If the masses of  $\Lambda$  and  $\Sigma$  were equal, one would expect the total  $\Sigma$  -number to be about 3 times the  $\Lambda_{\text{direct}}$  number, since each charge state has equal probability. Then the numbers would be approximately

$$\langle n_\Sigma \rangle \approx 3 \langle n_{\Lambda_{\text{direct}}} \rangle$$

$$\langle n_\Lambda \rangle \approx \langle n_{\Lambda_{\text{direct}}} \rangle + \frac{1}{3} \langle n_\Sigma \rangle = 2 \langle n_{\Lambda_{\text{direct}}} \rangle$$

$$\text{or } \langle n_\Sigma \rangle / \langle n_\Lambda \rangle \approx 3/2$$

This factor is nearly exactly compensated by the reduction of phase space coming from the higher mass of  $\Sigma$ .

Fig.18 Total number of  $\Xi^0, -$  per collision.

Fig.19 Total K-production per collision.

Fig.20 Total  $\bar{K}$ -production per collision.

Fig.21 The ratio  $K/\bar{K} \approx K^+/K^-$ . Since the K-mesons are produced in associated ( $N+N \rightarrow Y+K+n\pi$ ) and in pair production ( $N+N \rightarrow K+\bar{K}+n\pi$ ), whereas the  $\bar{K}$  are produced only in the latter reaction, this ratio is  $> 1$ . In fact, it rather strongly depends on  $\Omega_K$  in the "global symmetry" version and is constant in the version  $\Omega_Y = \Omega_K$ . If the experiment shows that  $K/\bar{K} \gg 1$ , then this definitely rules out the version (ii)  $\Omega_Y = \Omega_K$  in favour of the other one.

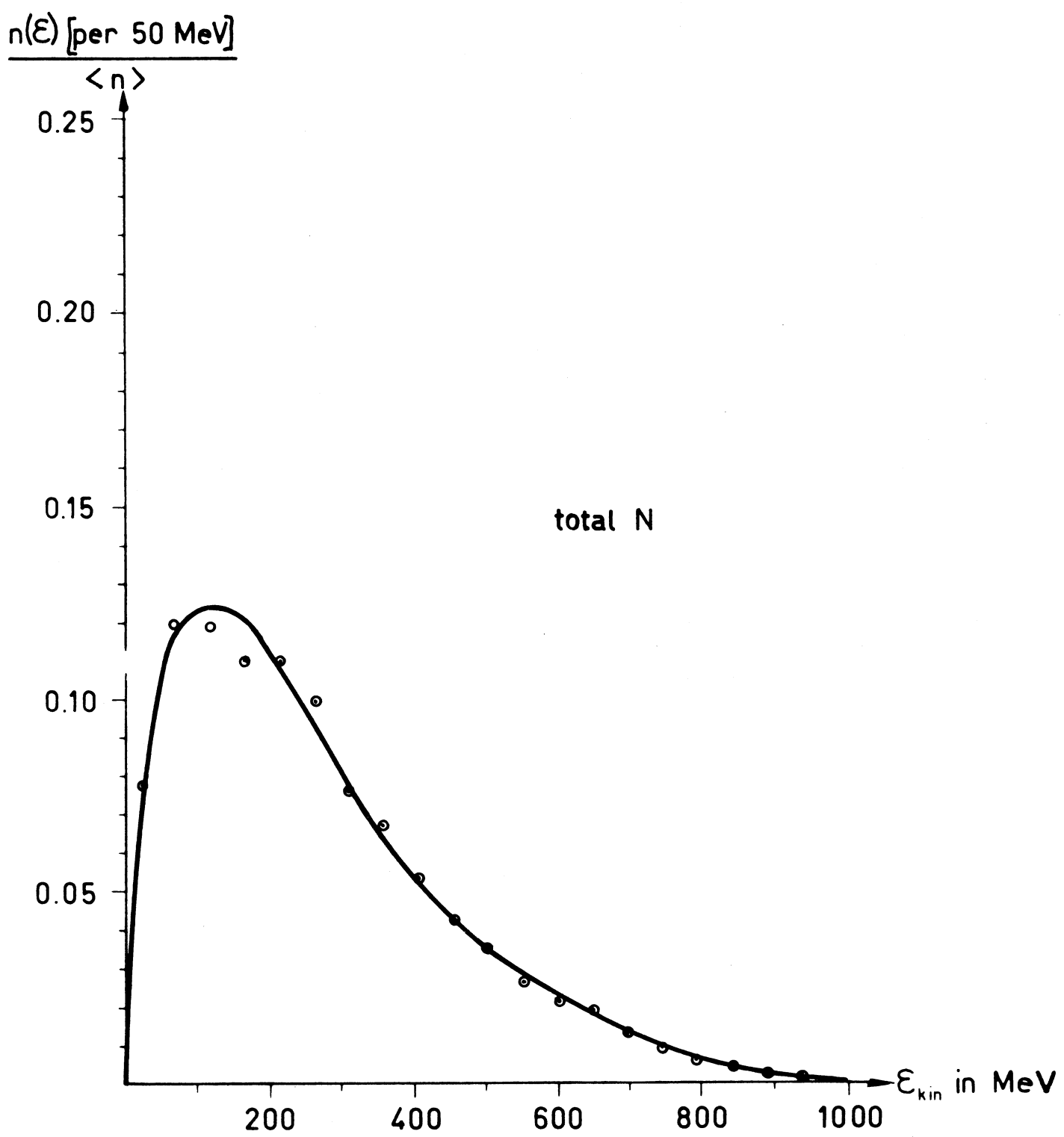


Fig. 1 Total nucleon spectrum

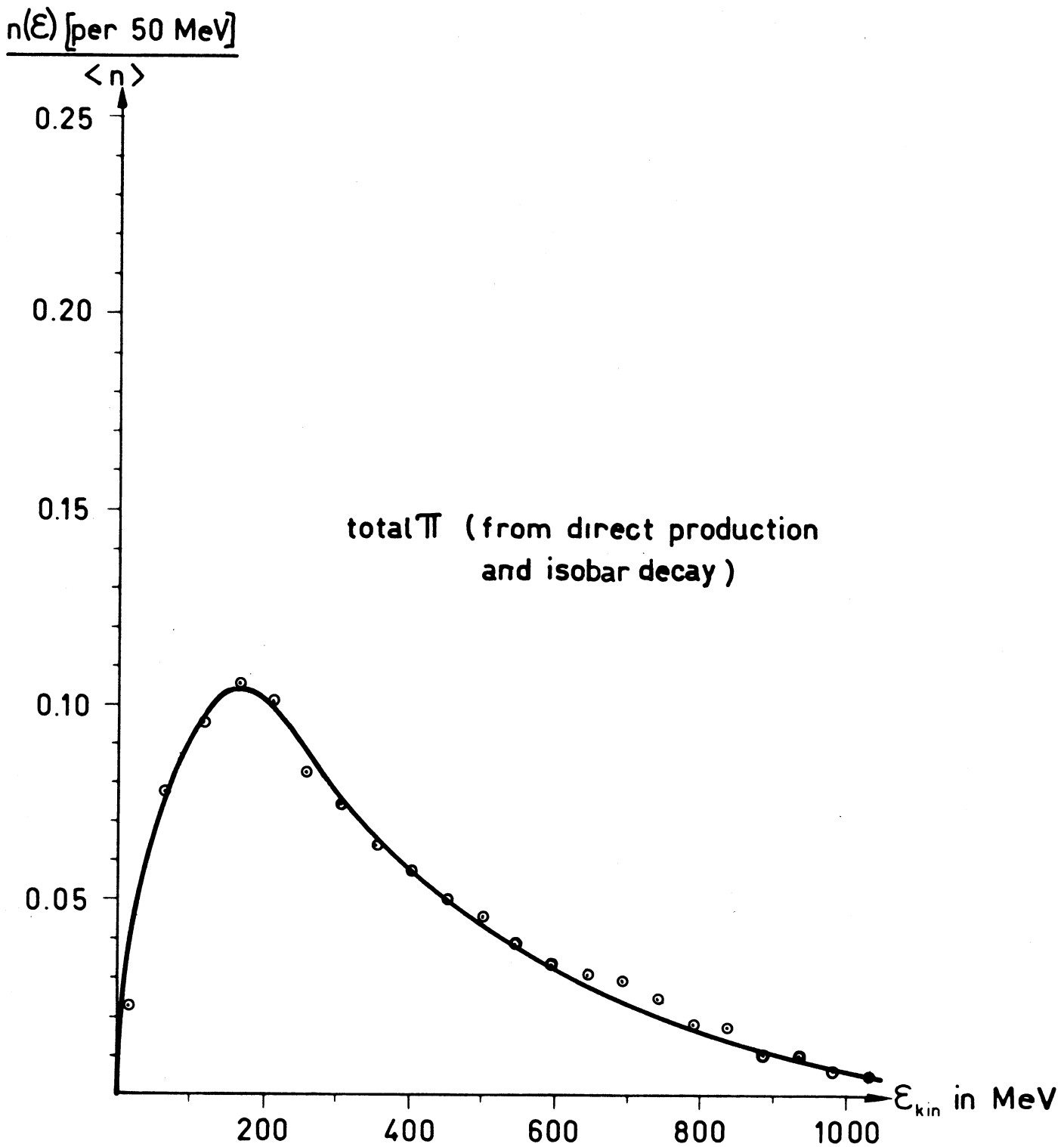


Fig. 2 Total  $\pi$ -spectrum.

The peak at low energy is mainly due to the decaying  $N^*$  (compare Fig. 3). The  $\pi^+$  and  $\pi^-$  spectrum will look similar except for the high-energy tail, where the charge-state probabilities are different for  $\pi^+$ ,  $\pi^0$  and  $\pi^-$ .

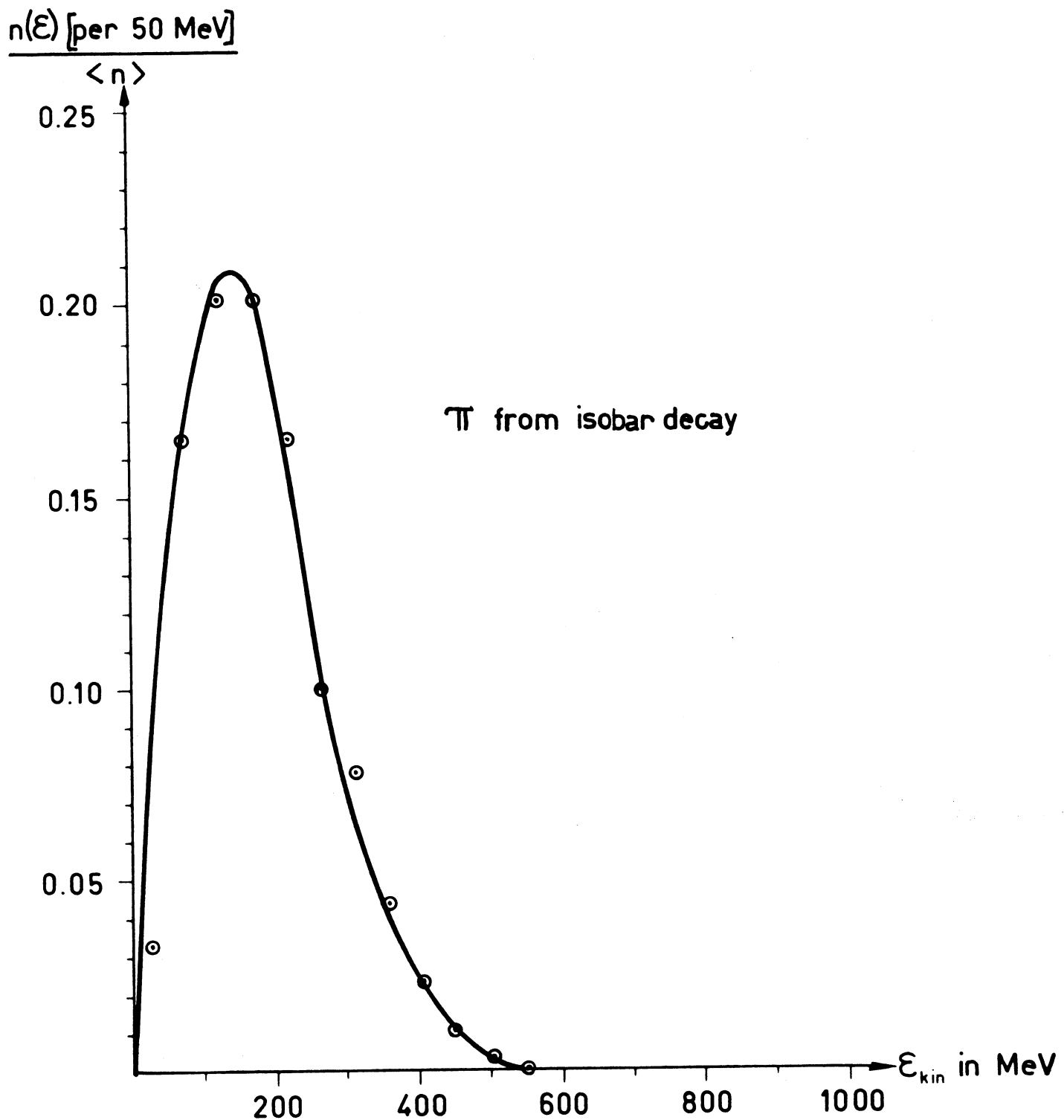


Fig. 3 The  $\pi$ -mesons coming from the decaying isobar.

$n(\varepsilon)$  [per 50 MeV]

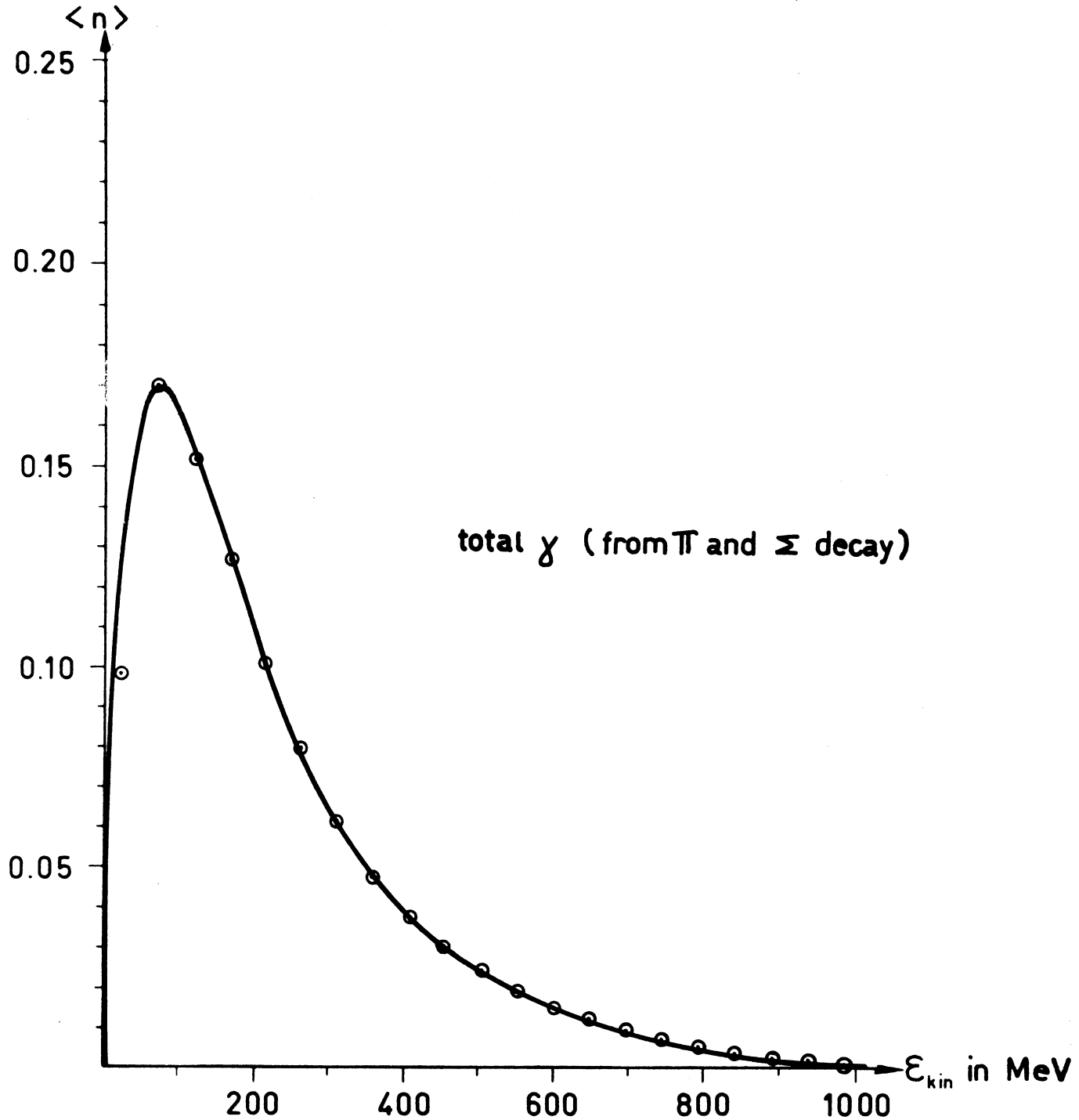


Fig. 4 The total  $\gamma$ -spectrum coming from  $\pi^0 \rightarrow 2\gamma$  and  $\Sigma^0 \rightarrow \Lambda + \gamma$   
Other  $\gamma$ -processes are not contained herein.

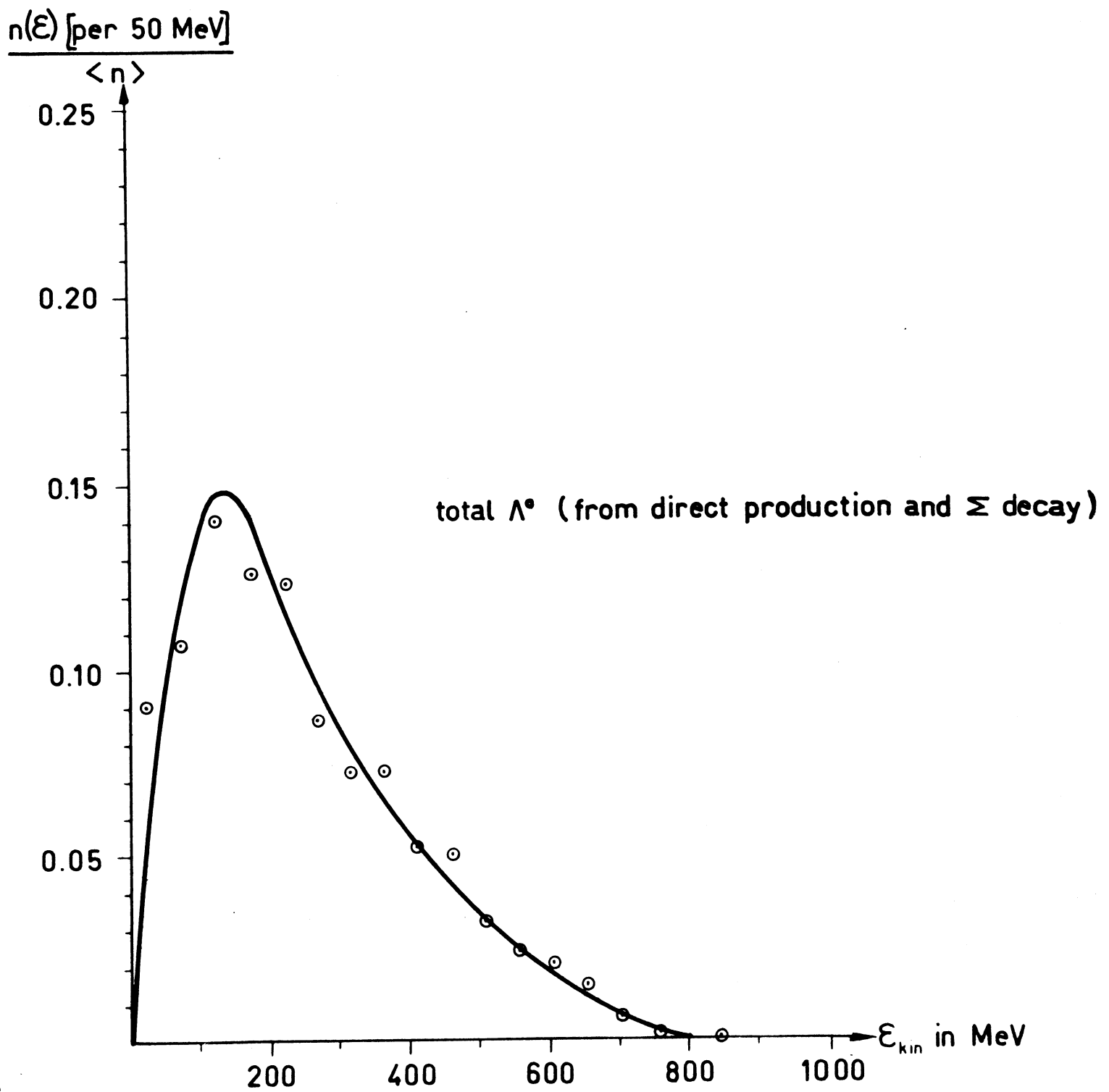


Fig. 5 Total  $\Lambda$  -spectrum, including  
 the decay of  $1/3$  of the produced  $\Sigma$ .

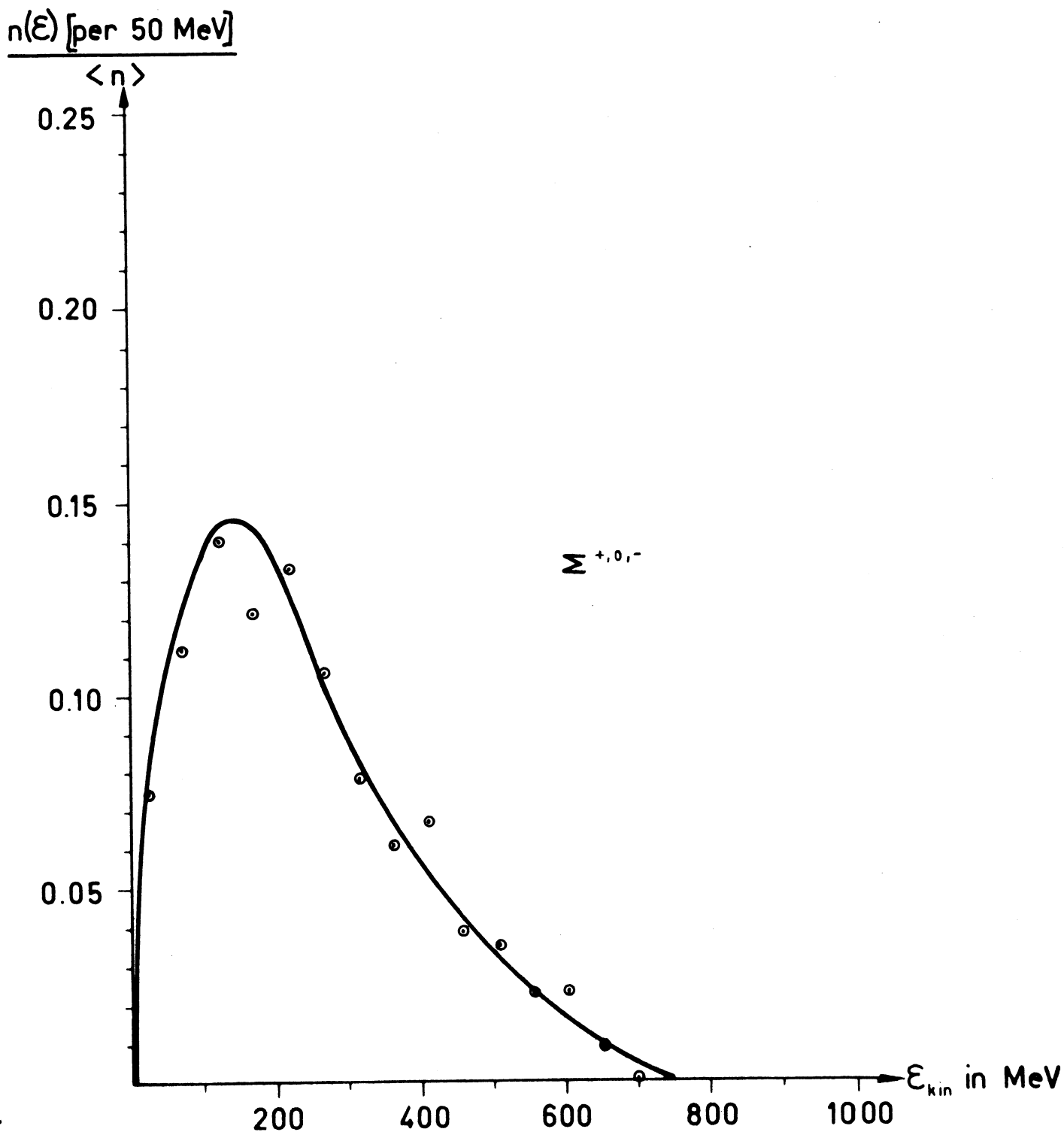


Fig. 6 Total  $\Sigma$  spectrum. The spectra for  $\Sigma^+$  and  $\Sigma^-$  may be somewhat different, in particular for the higher energies.

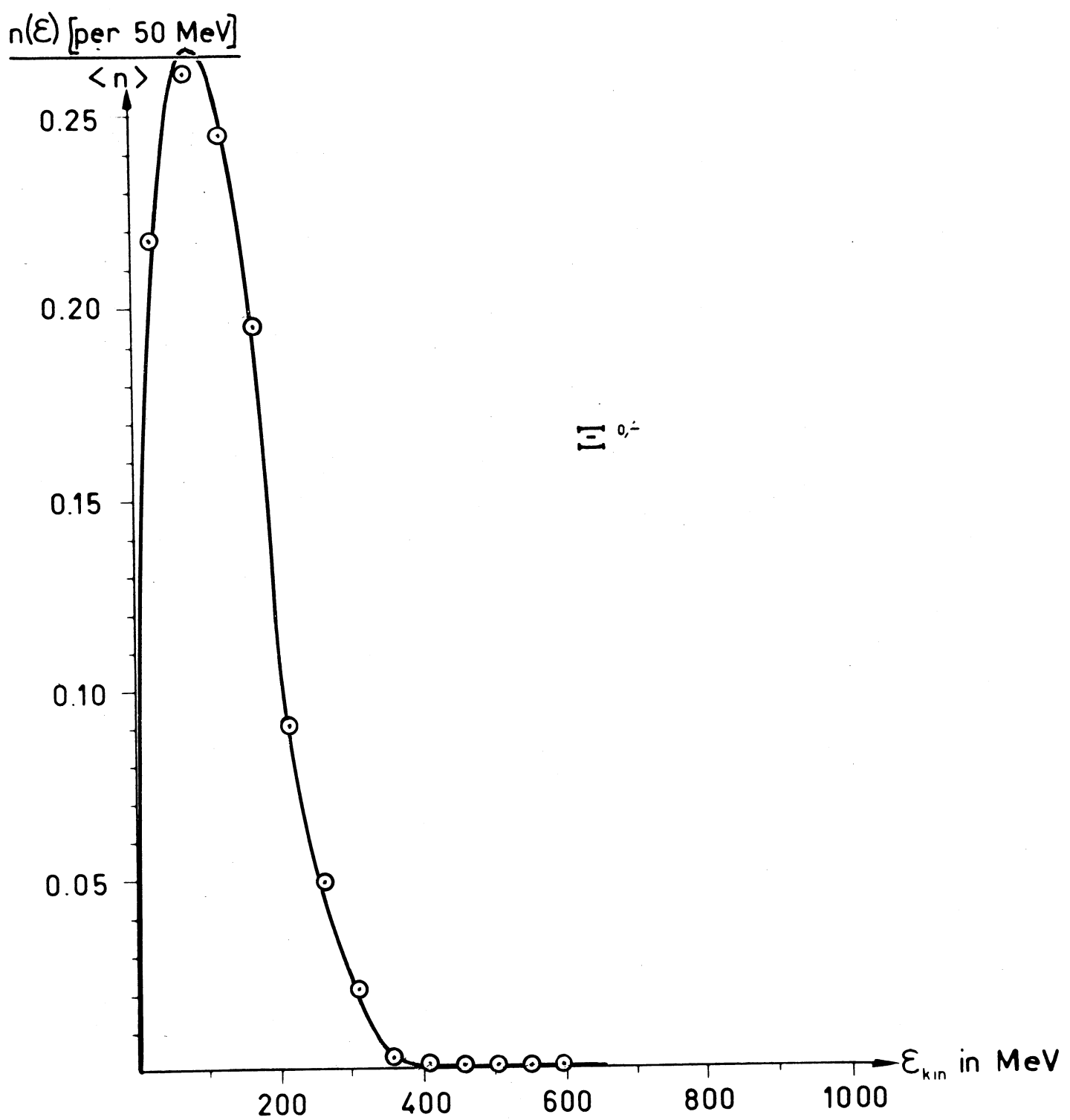


Fig. 7

The total  $\Sigma$ -spectrum.

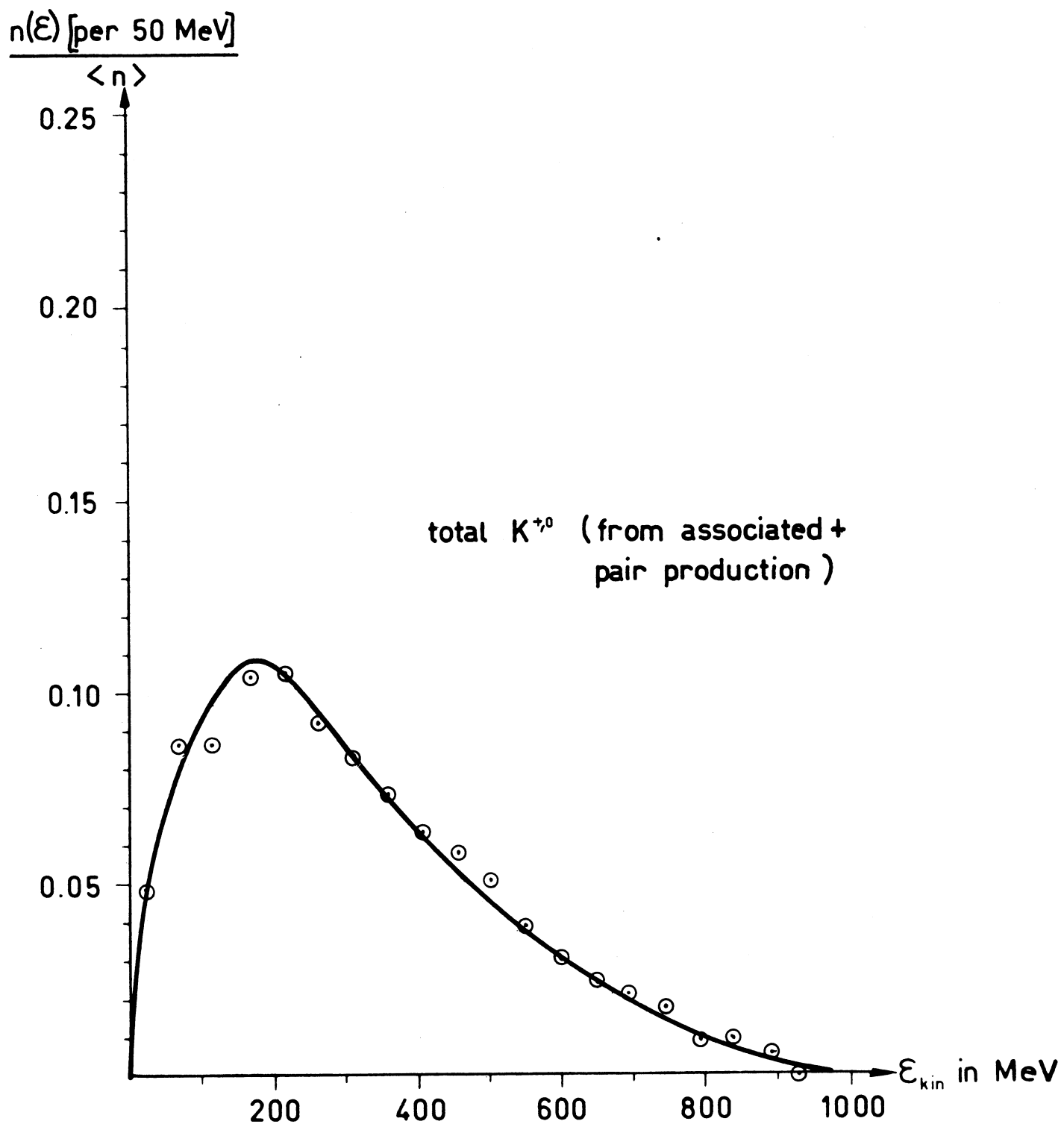


Fig. 8      Total K - spectrum.  
 To this the K mesons from  
 associated production and those  
 from pair production contribute.

$n(\epsilon)$  [per 50 MeV]

$\langle n \rangle$

0.25

0.20

0.15

0.10

0.05

$\bar{K}^{0,-}$

200

400

600

800

1000

$\epsilon_{kin}$  in MeV

Fig. 9

$\bar{K}$  - spectrum. Only  $K\bar{K}$  - pair production contributes. Note the different shape as compared with Fig. 8.

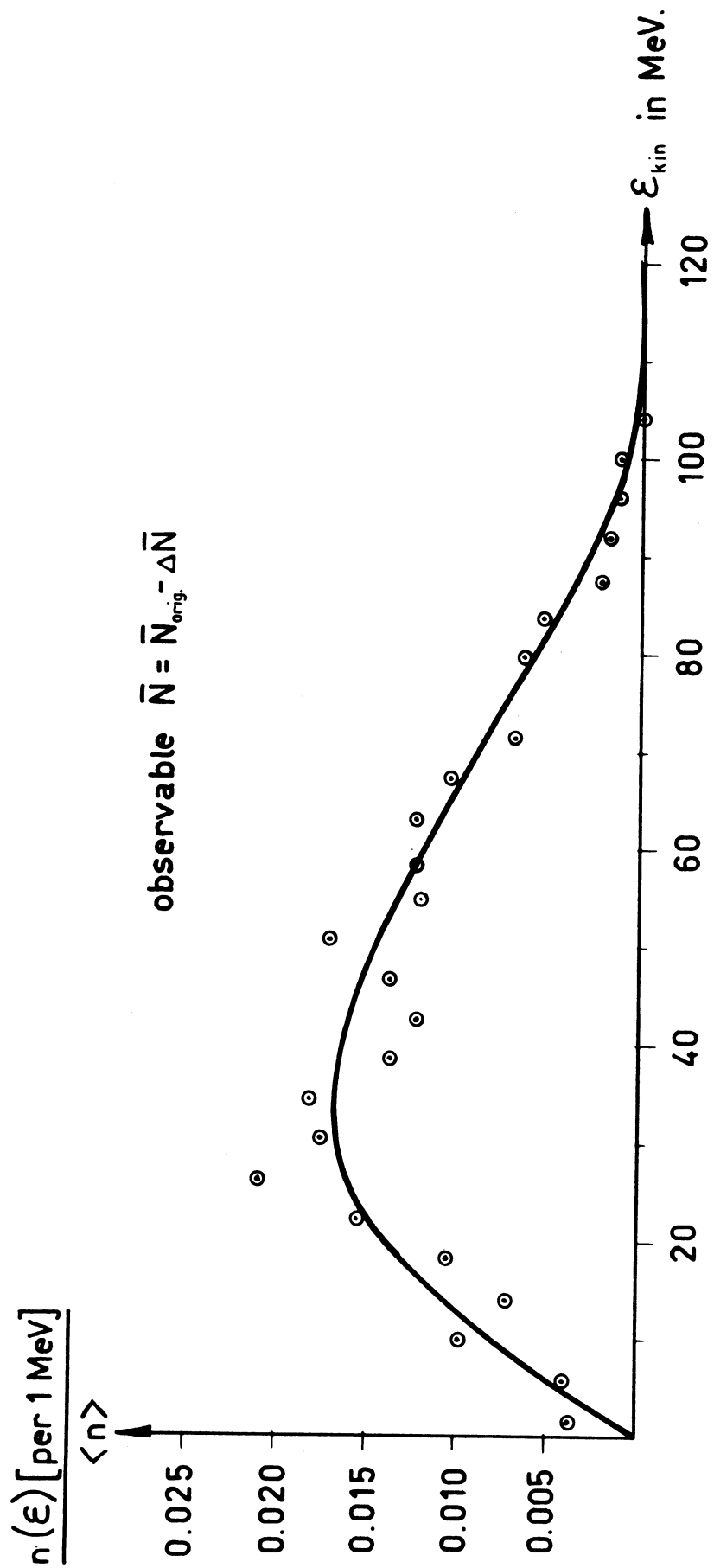


Fig. 10 Observable anti-nucleon spectrum, assuming final state annihilation.

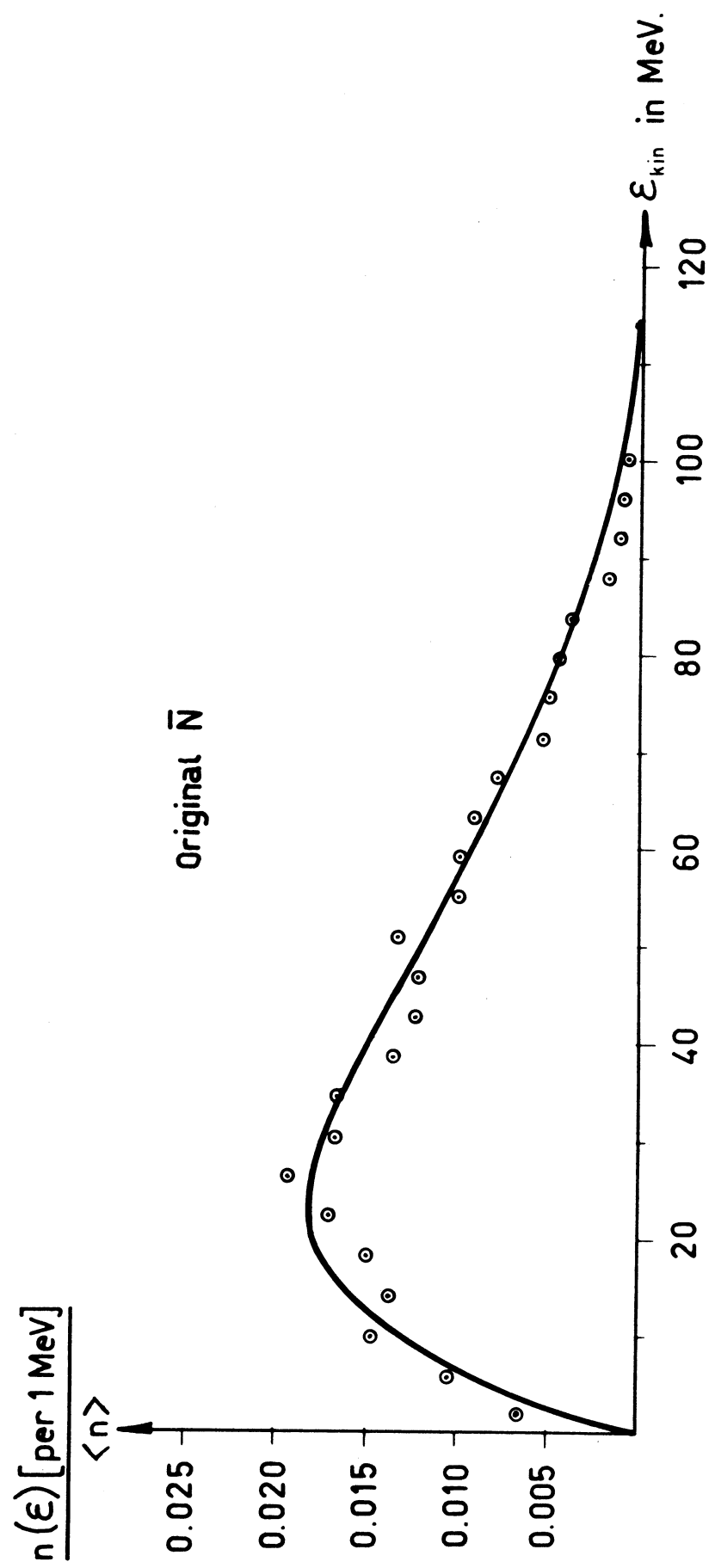


Fig. 11

Original anti-nucleon spectrum,  
without final state annihilation.

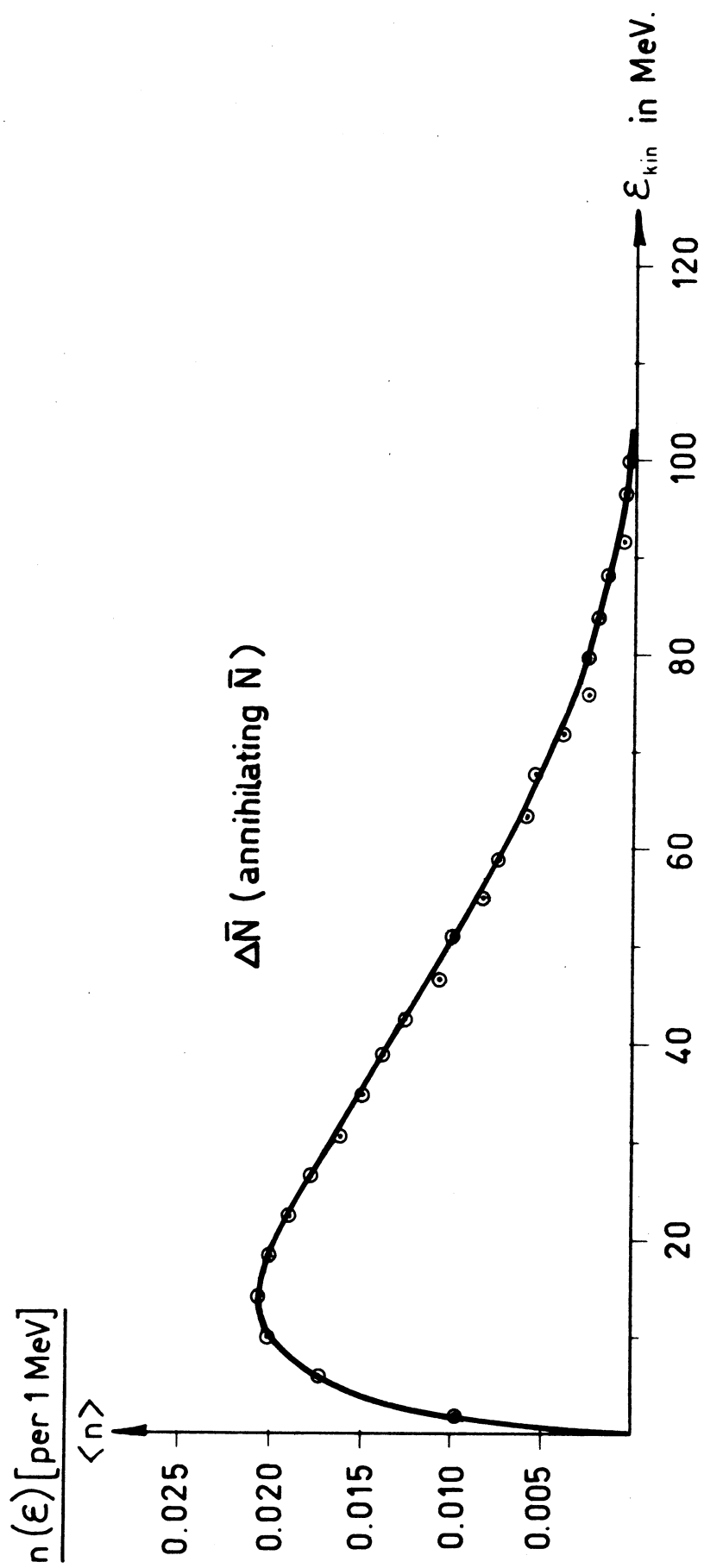


Fig. 12 Spectrum of those anti-nucleons, which have a chance to annihilate in final state. This spectrum, with a proper weight factor is subtracted from the original  $\bar{N}$  - spectrum, giving that of Fig. 10.  
Note that all three spectra are normalized to unity.

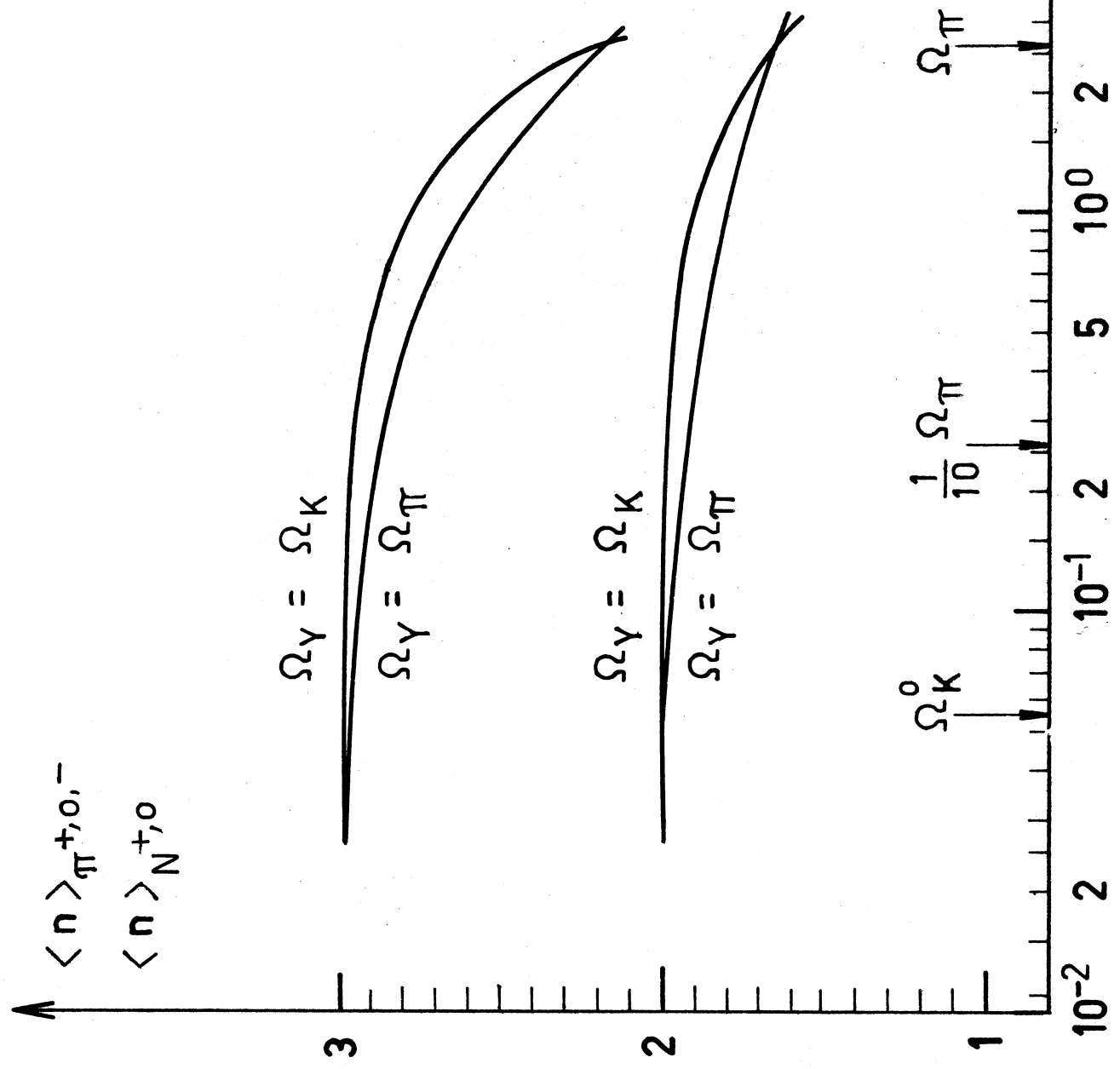


Fig.13

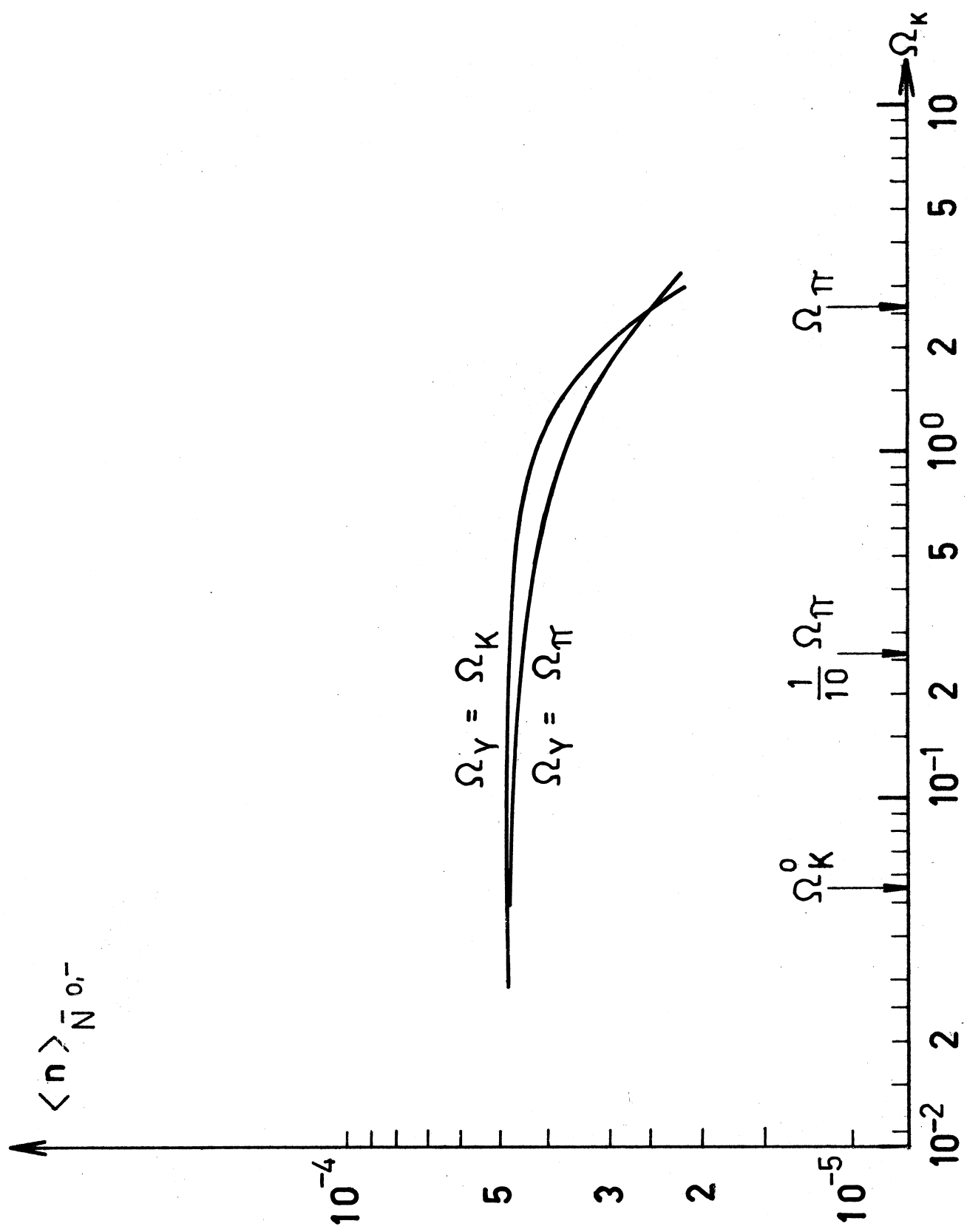


Fig. 14

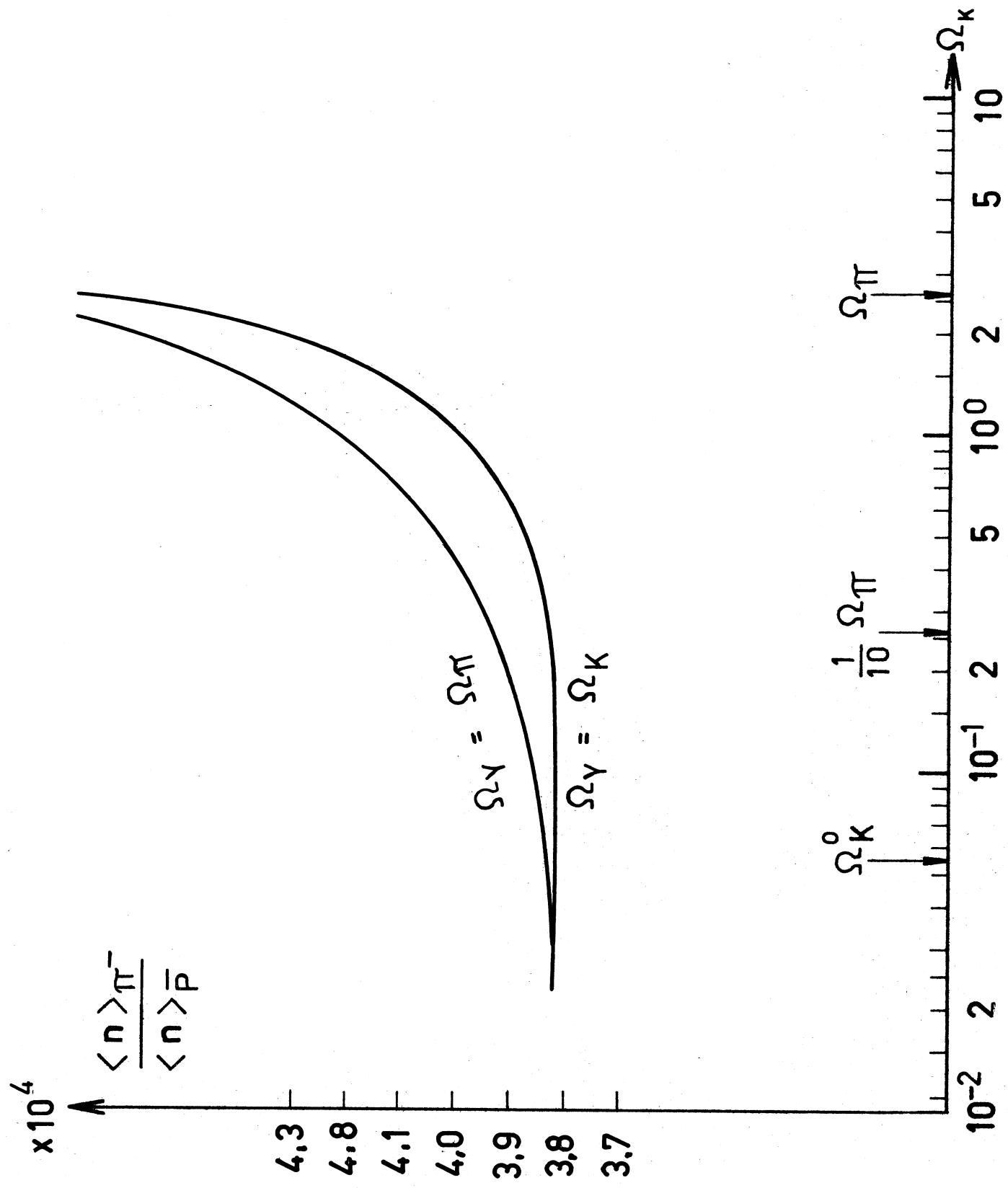


Fig. 15

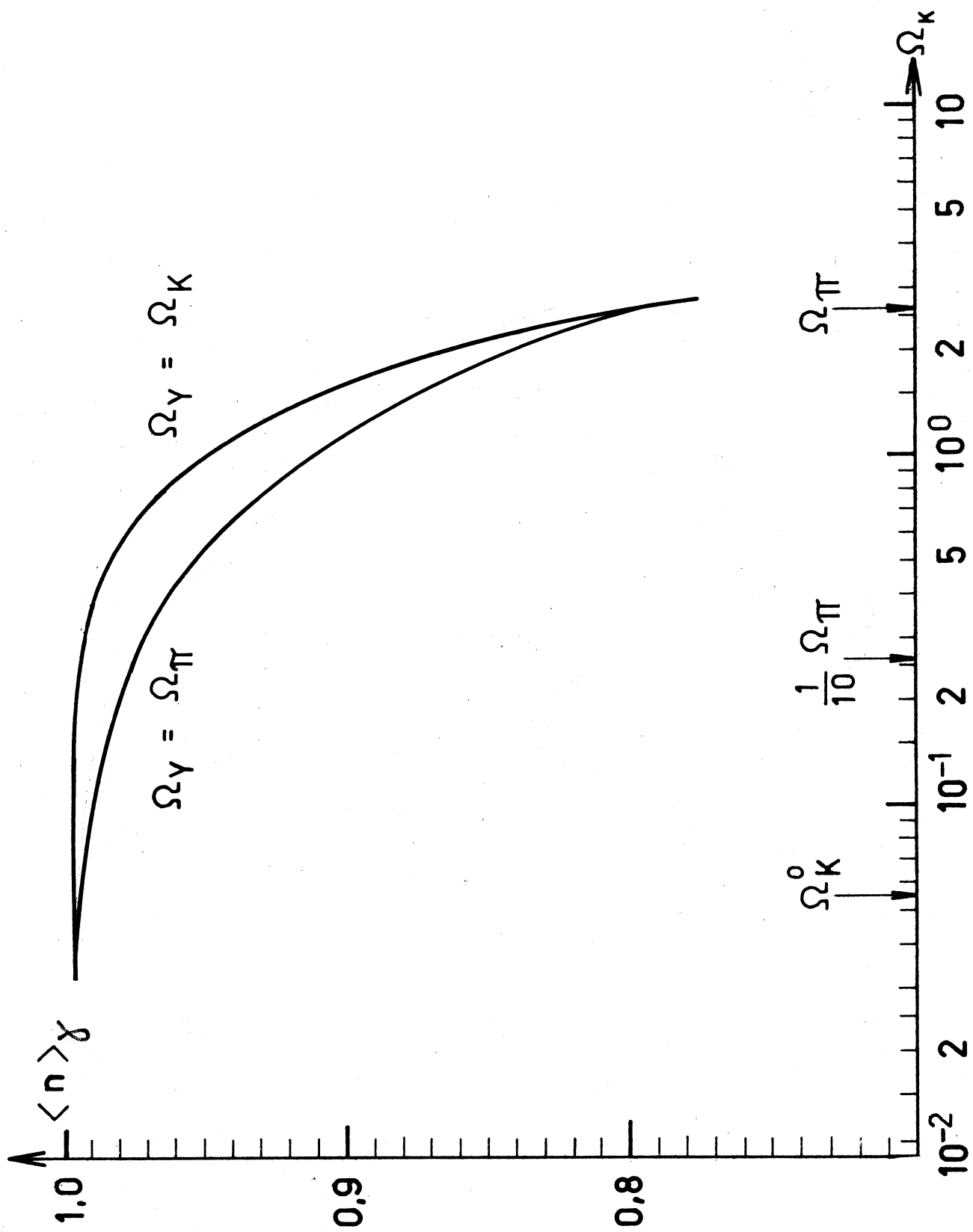


Fig. 16

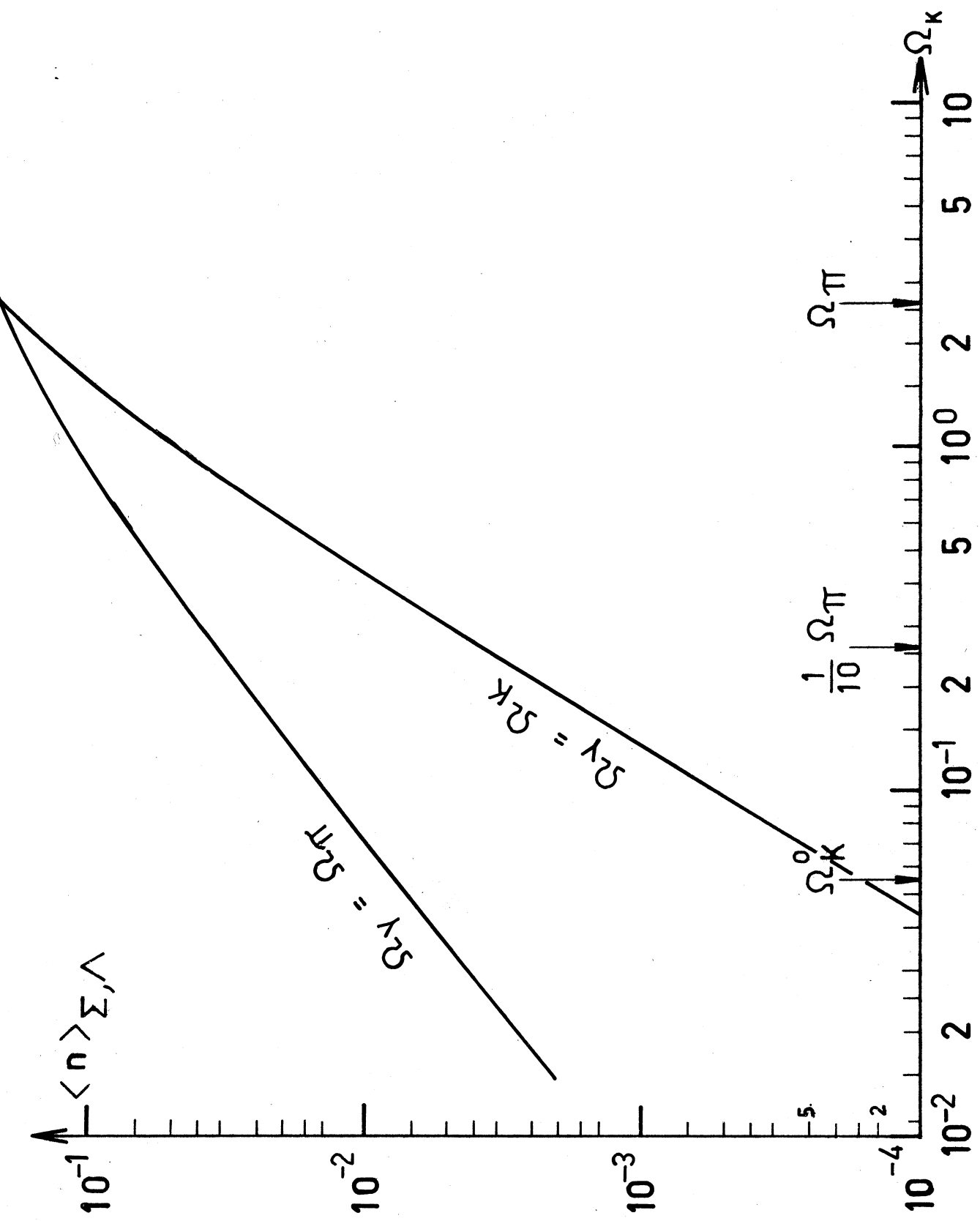
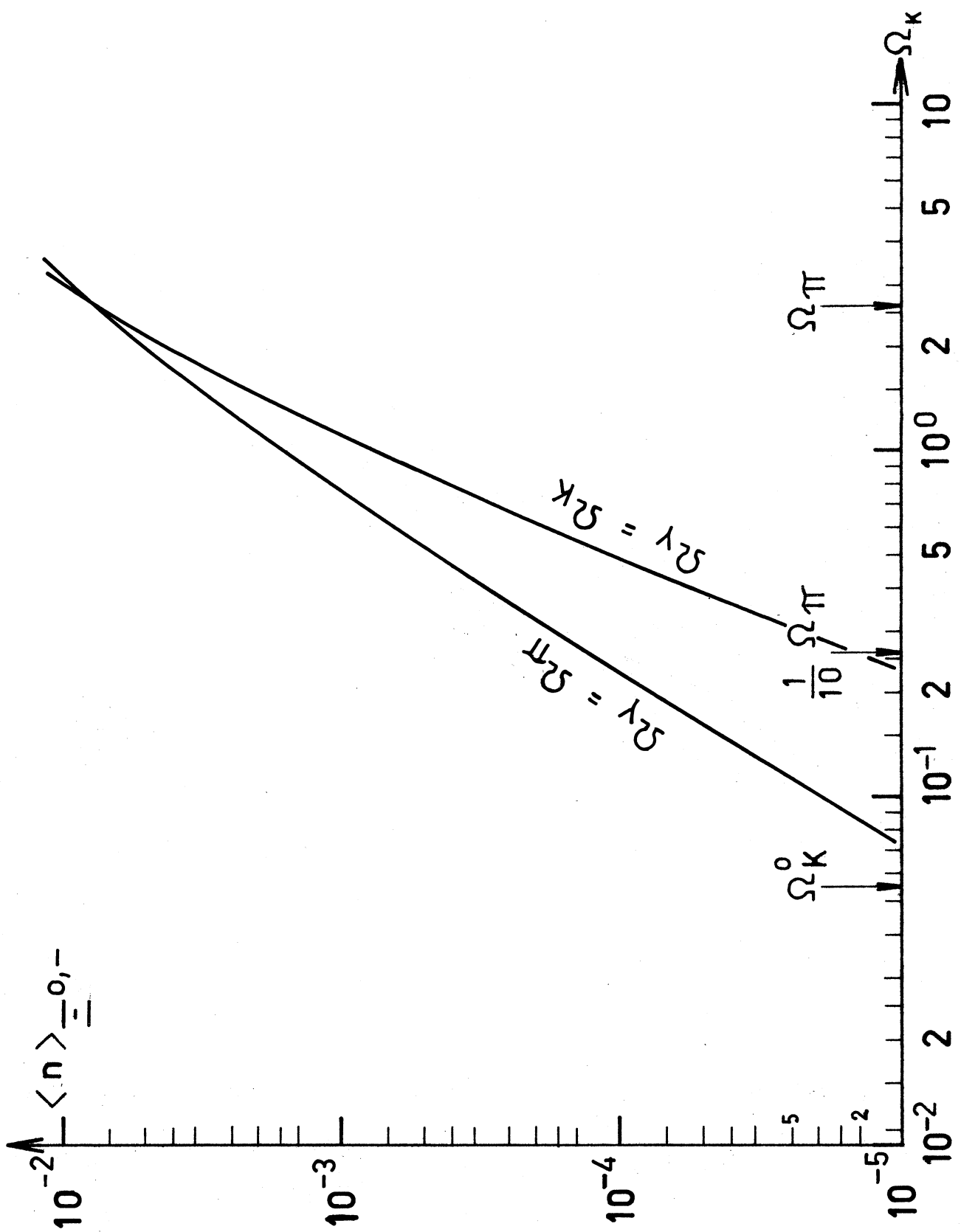


Fig. 17

Fig. 18



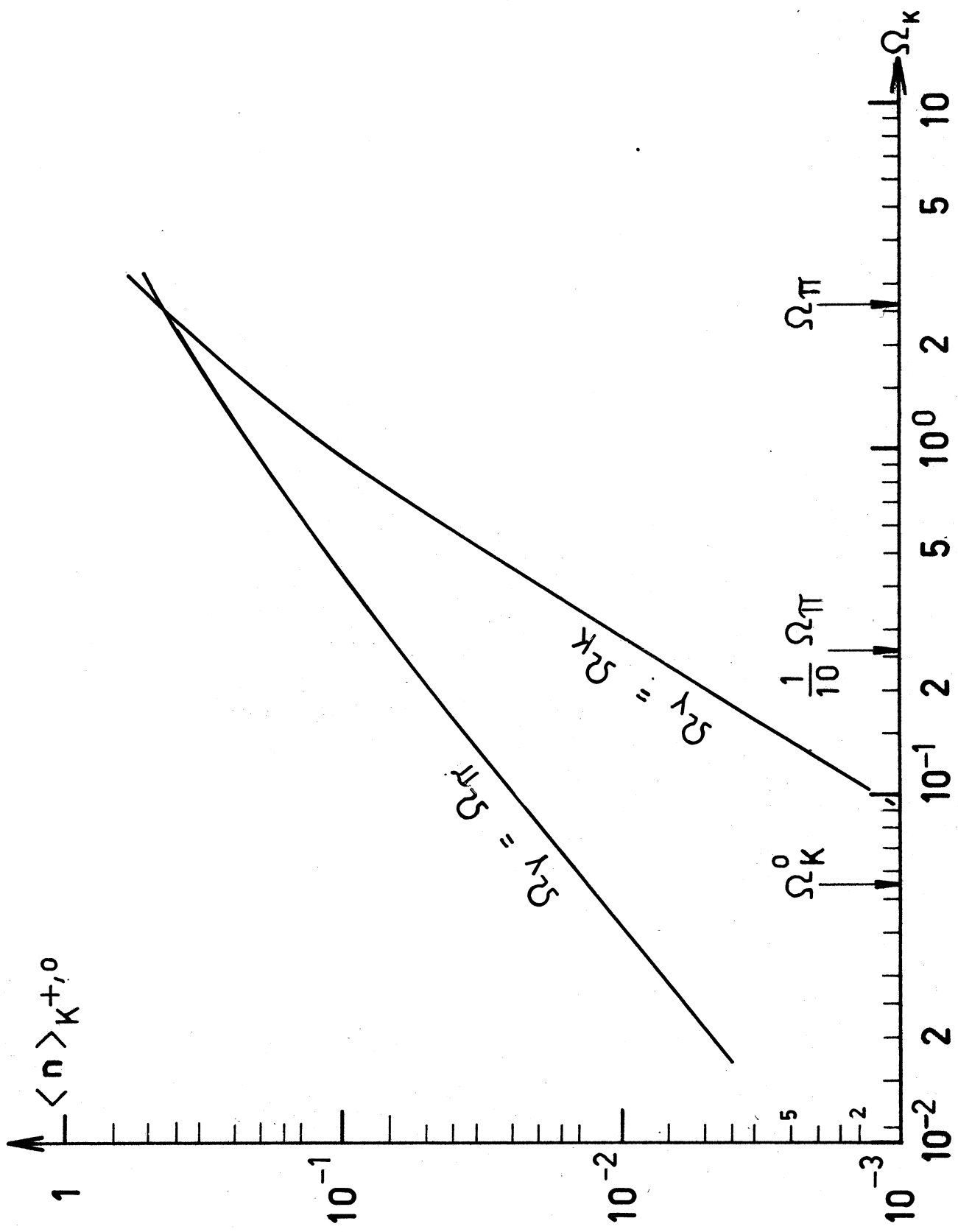


Fig. 19

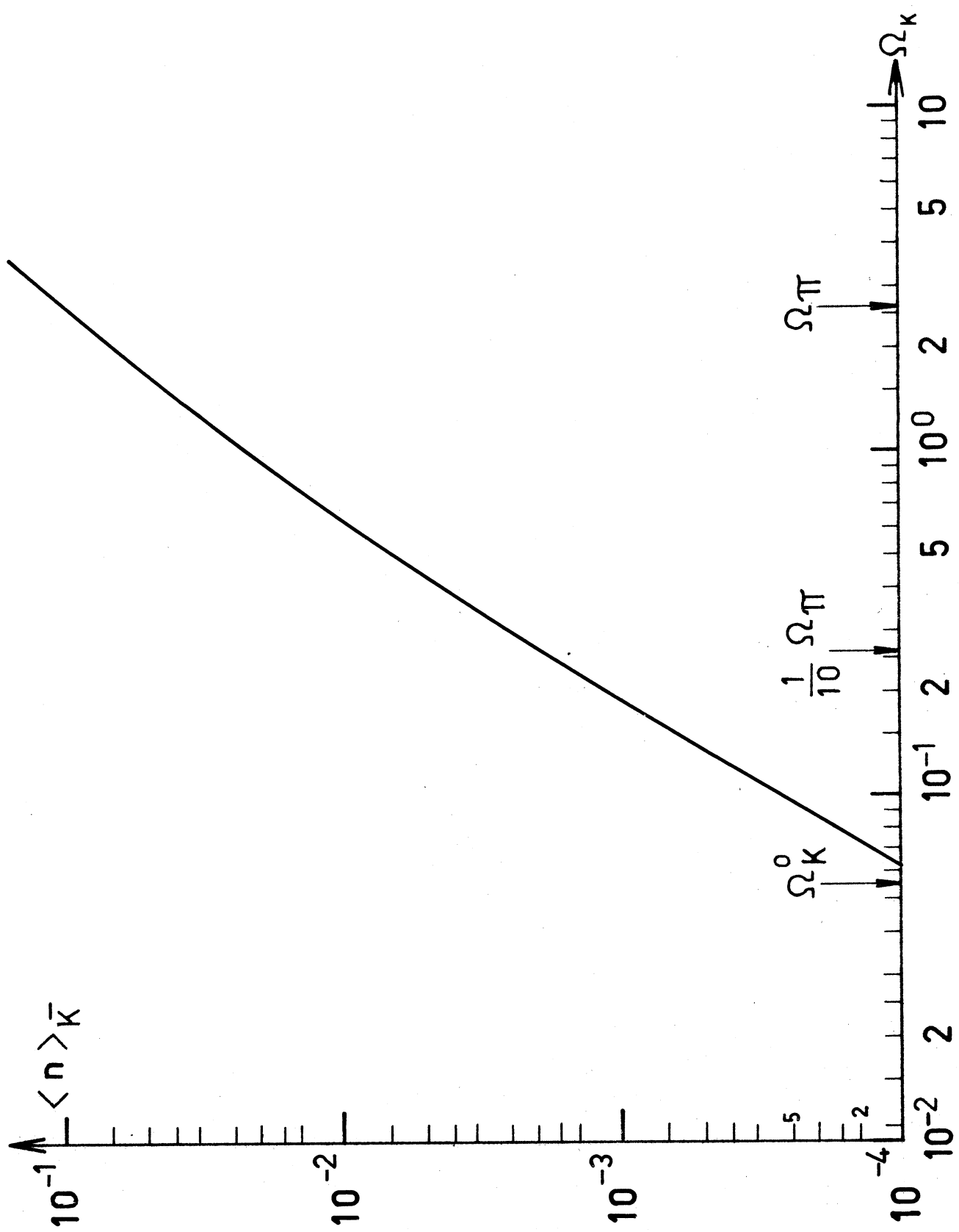


Fig. 20

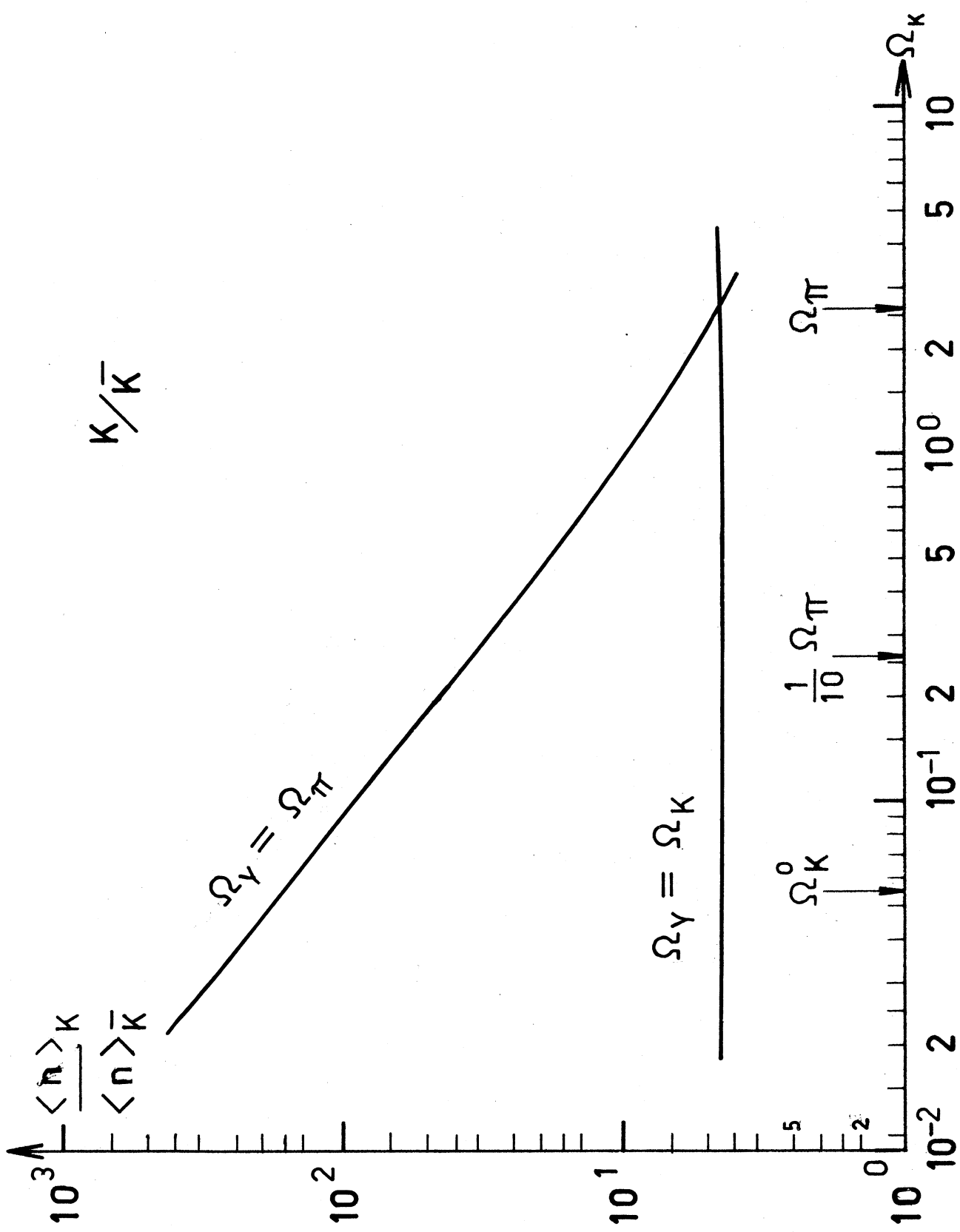


Fig. 21